Non-permissive SARS-CoV-2 infection of neural cells in the developing human brain and neurospheres

Running title: SARS-CoV-2 infection in the developing brain

Carolina da S. G. Pedrosa[1]*, Livia Goto-Silva[1]*, Ismael C. Gomes[2], Leticia R. Q. Souza[1], Gabriela Vitória[1], Isis M. Ornelas[1], Karina Karmirian[1,2], Mayara A. Mendes[1], José Alexandre Salerno[1,2], Teresa Puig-Pijuan[1,3], Carla Veríssimo[2], Jairo R. Temerozo[4,5], Daniel R. Furtado[1], Helena L. Borges[2], Thiago Moreno L. Souza[6,7], Marília Zaluar P. Guimarães [1,2] and Stevens Rehen[1,2].

1 - D'Or Institute for Research and Education (IDOR), Rio de Janeiro, RJ, Brazil.

2 - Institute of Biomedical Sciences, Federal University of Rio de Janeiro (UFRJ), Rio de Janeiro, RJ, Brazil.

3 - Carlos Chagas Filho Institute of Biophysics, Federal University of Rio de Janeiro (UFRJ), Rio de Janeiro, RJ, Brazil.

4 - National Institute for Science and Technology on Neuroimmunomodulation (INCT/NIM), Oswaldo Cruz Institute (IOC), Oswaldo Cruz Foundation (Fiocruz), Rio de Janeiro, RJ, Brazil.

5 – Thymus Research Laboratory, Oswaldo Cruz Institute (IOC), Oswaldo Cruz Foundation (Fiocruz), Rio de Janeiro, RJ, Brazil.

6 - Immunopharmacology Laboratory, Oswaldo Cruz Institute (IOC), Oswaldo Cruz Foundation (Fiocruz), Rio de Janeiro, RJ, Brazil.

7- National Institute for Science and Technology on Innovation in Diseases of Neglected Populations (INCT/IDPN), Center for Technological Development in Health (CDTS), Oswaldo Cruz Foundation (Fiocruz), Rio de Janeiro, RJ, Brazil.

8- Program of Immunology and Inflammation, Federal University of Rio de Janeiro (UFRJ), Rio de Janeiro, RJ, Brazil.

* These authors contributed equally to this work

Corresponding author: Stevens Rehen (srehen@lance-ufrj.org)

Abstract

Coronavirus disease 2019 (COVID-19) was initially described as a viral infection of the respiratory tract. It is now known, however, that many other biological systems are affected, including the central nervous system (CNS). Neurological manifestations such as stroke, encephalitis, and psychiatric conditions have been reported in COVID-19 patients, but its neurotropic potential is still debated. Here, we investigate the presence of SARS-CoV-2 in the brain from an infant patient deceased from COVID-19. The susceptibility to virus infection was compatible with the expression levels of viral receptor ACE2, which is increased in the ChP in comparison to other brain areas. To better comprehend the dynamics of the viral infection in neural cells, we exposed human neurospheres to SARS-CoV-2. Similarly to the human tissue, we found viral RNA in neurospheres, although viral particles in the culture supernatant were not infective. Based on our observations *in vivo* and *in vitro*, we hypothesize that SARS-CoV-2 does not generate productive infection in developing neural cells and that infection of ChP weakens the blood-cerebrospinal fluid barrier allowing viruses, immune cells, and cytokines to access the CNS, causing neural damage in the young brain.

Introduction

Severe acute respiratory syndrome coronavirus 2 (SARS-CoV-2) is the causative agent of the 2019 coronavirus disease (COVID-19), an airborne infectious disease. Most patients have symptoms of respiratory infections, such as fever, dry cough and dyspnea, with a subset of subjects evolving from a mild outcome to intensive care requirements and, in some cases, death. Respiratory failure is the main cause of death in COVID-19, because of the SARS-CoV-2 tropism to type II pneumocytes in the lungs, which also leads to the damage and sequelae observed in recovered patients (Meng et al., 2020).

Apart from respiratory symptoms, anosmia and ageusia were identified as hallmarks of COVID-19. Evidence for neurological disease associated with COVID-19 is increasing; in fact, 30 to 60% of patients further present one or more neurological symptoms, including paresthesia, altered consciousness, and headache (De Felice et al., 2020; Wang et al., 2020). Besides, COVID-19 patients are at a much higher risk to suffer stroke (7-fold), and 2-6% progress to cerebrovascular disease (Fifi and Mocco, 2020). Other less frequent neurological manifestations include encephalopathy, encephalitis and Guillain-Barré syndrome (Ellul et al., 2020; Mao et al., 2020).

Neuroinvasive behavior was shown for other highly pathogenic coronaviruses, including the Middle East Respiratory Syndrome coronavirus (MERS-CoV) (Li et al., 2016) and SARS-CoV (Glass et al., 2004; Xu et al., 2005). Similar to SARS-CoV, SARS-CoV-2 uses angiotensin-converting enzyme 2 (ACE2) as a cellular entry receptor (Yan et al., 2020). ACE2 is highly expressed in nasal epithelial cells, what underlies the respiratory tract infection (Sungnak et al., 2020), and is present in multiple tissues (Hamming et al., 2004).

Despite the aforementioned neuroinvasive potential of SARS-CoV-2, studies dissecting the mechanisms whereby the virus infects/replicates in the CNS are still scarce. SARS-CoV-2 infects non-neural cells in the olfactory epithelium in mice (Brann et al., 2020) and hamsters (Bryche et al., 2020). Additionally, it was inferred that sustentacular cells in the human olfactory epithelium expressing ACE2 are infected, in contrast to sensory neurons, which do not express these receptors (Brann et al., 2020).

Since viral infections targeting the brain were successfully modeled using human neurospheres and brain organoids (Garcez et al., 2016; Qian et al., 2016), researchers made use of these *in vitro* models to investigate whether SARS-CoV-2 infects the brain tissue, with contrasting results. While some suggested that the virus does indeed infect neurons and glia, others were unable to detect viral antigens in these cells (Jacob et al., 2020; Mesci et al., 2020; Pellegrini et al., 2020; Song et al., 2020). Nevertheless, from a

translational perspective, it is important to establish a dialogue between clinical and *in vitro* data. Here, we investigate SARS-CoV-2 infection in the postmortem developing human brain and in human neurospheres. Viral particles were mainly detected in the Choroid plexus (ChP) and Lateral Ventricle (LV), to a lesser degree in the human cerebral cortex, but not in the rest of the brain parenchyma. Viral infection was non-permissive in neurospheres suggesting that immune-mediated mechanisms, rather than the direct viral infection of neural cells, could be the cause for the tissue damage.

Results

SARS-CoV-2 infects the human brain

A case report from our group on the histopathological analyses of tissues from an infant deceased with COVID-19 and presenting neurological symptoms (Gomes et. al., submitted), prompted the question whether SARS-CoV-2 could directly infect the developing human brain. Samples from this patient were analyzed for viral presence, comparing different brain regions with each other and other affected organs (**Table 1**). Immunofluorescence (IF) staining with anti-SARS-CoV-2 spike protein (SP) was detected in ChP and LV lining, and in very few locations of the frontal cerebral cortex (**Figure 1A**). Other brain areas lacked immunostaining, as listed in Table 1 (**Supp Figure 1A**). The heart and the lung, which have been previously demonstrated to be infected by SARS-CoV-2 (Bradley et al., 2020; Mallapaty, 2020; Remmelink et al., 2020; Tabary et al., 2020), were also positively stained (**Table 1**, **Figure 1A**). Tissues from infants that did not die by COVID-19 have not shown SARS-CoV-2 spike protein staining confirming the specificity of the antibody (**Supp Figure 1B**). SARS-CoV-2 RNA was also observed in ChP, LV, frontal cortex and heart samples (**Figure 1B, Supp Table1**). These results indicate that the ChP and the LV could be a gateway to SARS-CoV-2 in the CNS, but that the virus does not efficiently spread into the brain parenchyma, as shown by the low levels of infection in the cortex and other regions adjacent to the lateral ventricle.

Table 1: Immunostaining for SARS-CoV-2 in tissues autopsied from a child deceased due to COVID-19.

Tissues	Status of SARS-Cov-2 Staining
Brain	
Choroid Plexus	Positive
Lateral Ventricle	Positive
Frontal Cortex	Positive
Medulla oblongata	Negative
Pons	Negative
Midbrain (with cerebral aqueduct of Sylvius)	Negative
Putamen and Globus pallidus	Negative
Temporal lobe	Negative
Heart	Positive
Lung	Positive

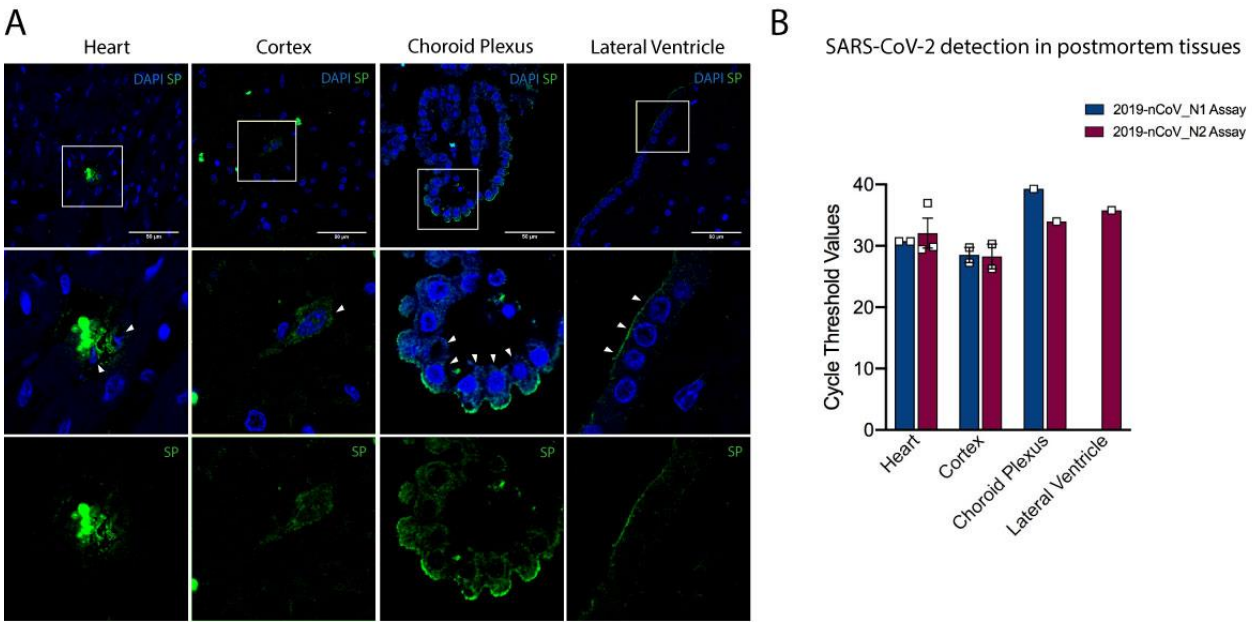

Figure 1. **SARS-CoV-2 identified in the heart, cerebral cortex and choroid plexus (ChP) of a child deceased due to COVID-19. (A)** IF staining in the heart, cortex and ChP tissues with anti-SARS-CoV-2 spike protein (SP). Calibration bar: 50 µm **(B)** Detection Results of human *postmortem* tissue samples by quantitative Reverse Transcriptase–Polymerase Chain Reaction (qRT-PCR). The bars represent average and standard error of cycle threshold value (Ct). Ct values less than 40 were interpreted as positive for SARS-CoV-2 RNA. Each square represents a distinct tissue fragment from the same tissue specimen.

Neural cells in both the developing cerebral cortex and neurospheres have lower expression of ACE2 than other tissues infected by SARS-CoV-2

Human neurospheres have been successfully used to model some aspects of viral infection in the brain tissue (Garcez et al., 2016). To confirm that neuronal and glial cells are not susceptible to a productive infection of SARS-CoV-2, we used neurospheres as an *in vitro* model for the developing brain. First, we verified if the expression levels of ACE2 would be comparable between *in vivo* and *in vitro*, relative to other non-neural tissues. We compared the expression levels of ACE2 in different brain regions to those IF-positive tissues using data from Protein Atlas and Allen Brain Atlas databases. The ChP has higher expression of ACE2 when compared to other brain regions (**Figure 2A**). Similarly to cerebral cortical tissues, human neurospheres have lower expression of ACE2 mRNA, when compared to human cardiomyocytes *in vitro* (**Figure 2B**), which have been previously demonstrated to be permissive to SARS-CoV-2 infection (Marchiano et al., 2020; Pérez-Bermejo et al., 2020). Neurospheres and cardiomyocytes *in vitro* reproduce the differences in the expression of ACE2 described in the *in vivo* databases (**Figure 2**).

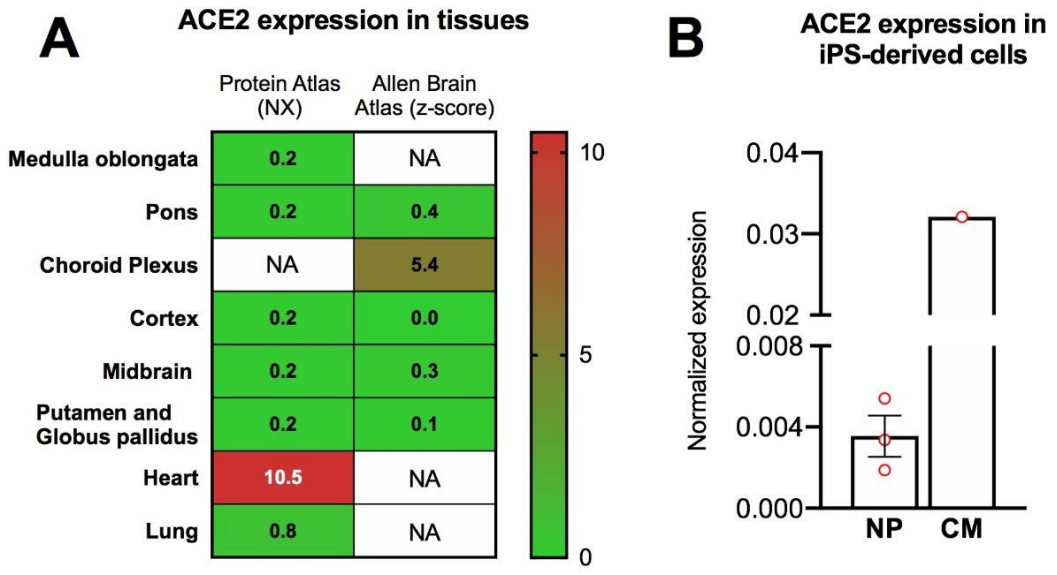

Figure 2. ACE2 expression in human tissues and iPSC-derived cells. (A) ACE2 expression in human tissues based on Protein Atlas and Allen Brain Atlas databases, with respective units. NA= not analyzed **(B)** Relative mRNA expression levels of ACE2 in iPSC-derived cells: neurospheres (NP) and cardiomyocytes (CM) (n=3 for NP and n=1 for CM).

Exposure of human neurospheres to SARS-CoV-2 elicits non-permissive infection

SARS-CoV-2-infection in neurospheres was addressed using the multiplicity of infection (MOI) of 0.1, which has been described to productively infect permissive cells, such as Vero and Calu-3 cells (Han et al., 2020; Lamers et al., 2020).

We were unable to detect SARS-CoV-2 in neurospheres at 5 days post infection (d.p.i.) using antibodies for double-stranded (ds)RNA (**Figure 3A**). On the other hand, neurospheres were successfully infected with Zika virus, showing dsRNA staining (arrows) (**Figure 3A**), confirming the efficiency in detecting replicative viral RNA. Consistently, SARS-CoV-2 could be efficiently detected in infected Vero cells (MOI 0.01) using dsRNA antibody and CS (**Figure 3A and Supp Figure 2)**. Corroborating these results, no viral proteins were detected in western blotting (WB) of neurospheres obtained at 2 d.p.i., using neither anti-SARS-CoV-2 CS nor the monoclonal anti-SARS-CoV-2 SP (**Figure 3B**). In contrast, WB of infected Vero cells show prominent bands corresponding to the molecular weight of SARS-CoV-2 nucleoprotein and SARS-CoV-2 spike protein, by reacting with anti-SARS-CoV-2 CS and anti-SARS-CoV-2 SP, respectively (**Figure 3B, +CTRL**).

Similar to the observations in the cerebral cortex, low levels of viral RNA could be detected in the supernatant of neurospheres. After 5 d.p.i., neurosphere's supernatant had as few as 10^5 copies of subgenomic SARS-CoV-2 RNA, which suggests that SARS-CoV-2 is able to transcribe its RNA in neuronal cells , however, with much less efficacy than Vero cells **(Figure 3C**). Then, a plaque forming unit (PFU) assay was performed to address the infectivity of the virus in the supernatant of neurospheres. The analysis of the supernatant after 1h of virus inoculum exposure showed about 3 x 10^3 PFU/mL, confirming that neurospheres were exposed to infectious virus particles (**Figure 3D, Day 0)**. At 2 and 5 d.p.i, human neurospheres were unable to produce infective viral progenies (**Figure 3D**). The aforementioned detection of virus RNA contrasts with the absence of infectious virus progeny and may indicate that neural cells were led to a dead-end abortive SARS-CoV-2 infection.

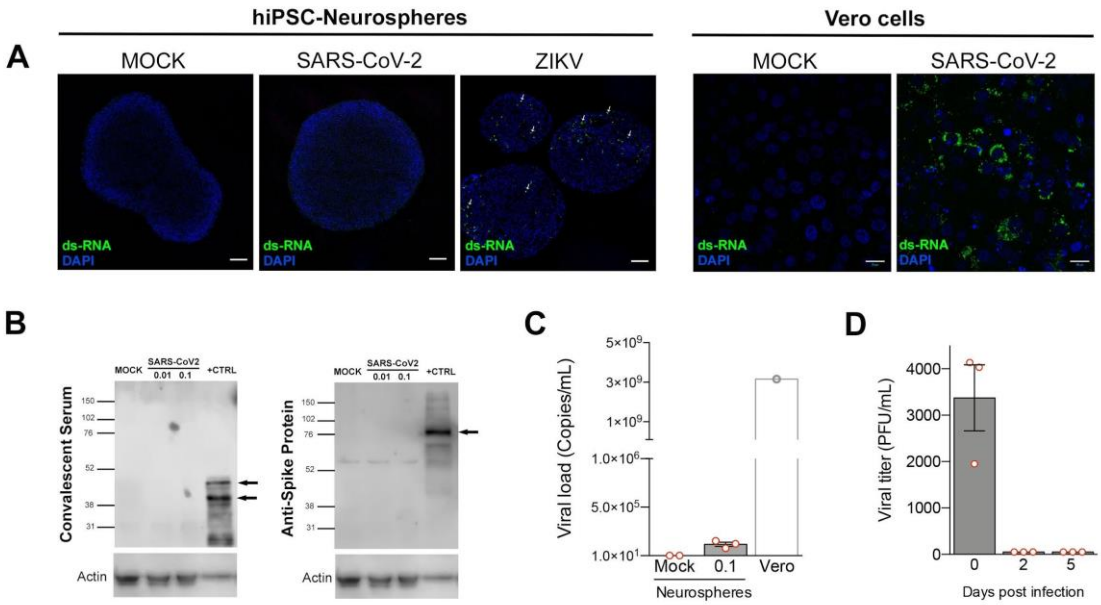

Figure 3. ***SARS-CoV-2 elicits unproductive infection in human neurospheres.*** Human neurospheres were exposed to SARS-CoV-2 (MOI 0.1) for 5 days. On days 2 and 5 post-infection neurospheres and their supernatants were recovered for analysis. **(A)** IF staining for SARS-CoV-2, with anti-dsRNA (green) in cryosections of 5 d.p.i neurospheres. Nuclei were counterstained with DAPI (blue). Zika Virus-infected neurospheres and SARS-CoV-2-infected Vero cells were used as staining control (n=3). Calibration bar: 50 µm for neurospheres and 20 µm for Vero cells. **(B)** Western blot for SARS-CoV-2 proteins with detection by anti-SARS-CoV-2 CS or anti-SARS-CoV-2 SP. Protein extracts from Vero cells (MOI 0.1 for 24h) were used as positive control. Gel loading was assessed with beta-actin staining (n=2) **(C)** Real-time qRT-PCR of subgenomic RNA levels of SARS-CoV-2 in the supernatants of neurospheres 5 d.p.i (n=3) and Vero cells for comparison. Regarding the latter cell type, plotted is the average value of results submitted elsewhere (Sacramento et al, submitted). **(D)** Plaque forming units assay for the supernatants of the neurospheres. Data was plotted as average plus standard error (n=3).

Discussion

Neurological manifestations of COVID-19 fueled research of viral infection in the brain. However, absence or low detection of SARS-CoV-2 was described in the cerebrospinal fluid (CSF), whereas no viral particles have been localized in the human brain parenchyma (Espíndola et al., 2020; Schaller et al., 2020). Here, we report SARS-CoV-2 infection in the ChP and in its LV lining, and mild infection in the frontal cortex of an infant's brain (described in a detailed pathological analysis in Gomes et al., submitted) (**Figure 1A**). The infection was confirmed by IF and real time PCR quantification of viral RNA, applying CDC validated primers and assay conditions. Despite the limited availability of the *postmortem* tissues, the latter method successfully amplified N1 and N2 in some of the samples, as reported in the result section. Due to the limited amount and quality of tissue, especially in the ChP and LV samples, fewer replicates of amplifications were obtained in some cases (**Supp Table 2**). Nevertheless, since a false negative is the biggest caveat of unproper tissue preservation, and the results were positive with all the appropriate controls, and due to the fact that PCR results corroborate the IF, altogether we are confident of the presence of the virus in the cortex, ChP and LV.

ChP acts as a barrier separating the blood from the CSF (Lun et al., 2015; Javed et al., 2020). This barrier is also a site of virus entry and spread into CNS, as demonstrated by the infection of ChP's pericytes with ZIKV that invades the CNS (Kim et al., 2020). The ChP epithelial cells infected with human polyomavirus (JCPyV) produce extracellular vesicles that spreads towards glial cells (O'Hara et al., 2020). It was also proposed that the ChP is a site of infection of lentiviruses and enteroviruses and a reservoir of HIV in the CNS (Schwerk et al., 2015). It has already been shown that newborns may have early infection of the ChP with the Herpes Simplex virus (HSV1) and are more susceptible to encephalitis than adults, which is related to dampened interferon response in newborn's brains (Wilcox et al., 2016). This weakened response could explain the observation of SARS-CoV-2 in an infant brain. Virus infection in ChP elicits an immune response with the production of chemokines and cytokines and consequent alterations in the permeability of the blood-CSF barrier, which enables the invasion of immune cells of the CSF into the CNS that could become harmful. The presence of SARS-CoV-2 is enhanced in epithelial cells of the ChP, sparse in LV and cortex, and undetectable in other brain regions, suggesting that the described neurological manifestations are likely due to collateral effects of a systemic immunological response to the virus.

The presence of SARS-CoV-2 is more pronounced in the ChP than in the cortex. This matches expression data for the SARS-CoV receptor ACE2, which is enriched in ChP

both *in vivo* and *in vitro*, in comparison to other brain areas, including cortex (Jacob et al., 2020; Pellegrini et al., 2020) (**Figure 2**). Our protocol for differentiating neurospheres generates cortical brain-like tissue (Garcez et al., 2017) which recapitulates the low expression levels of ACE2 mRNA observed in the human cortical tissue (**Figure 2B**). ACE2 levels are increased in patients with comorbidities, suggesting a relationship between ACE2 expression and susceptibility to severe COVID-19 (Pinto et al., 2020). Strategies to regulate the expression of ACE2 have been proposed as therapies to fight viral infection (Annweiler et al., 2020; Liu et al., 2020). Also, it remains unaddressed if neuropsychiatric conditions and neurodegenerative diseases impact the expression of ACE2 in the brain (Rocha et al., 2018) and how they could interfere with the susceptibility of CNS infection. Indeed, there is an increased risk for psychiatric disease in COVID-19 patients, especially those which had previous psychiatric episodes (Mazza et al., 2020). In this context, human neurospheres and brain organoids could play a role for *in vitro* drug testing, being useful to monitor changes in ACE2 expression along with susceptibility to SARS-CoV-2 infection.

One experimental aspect that drew our attention was the amount of virus used to infect cells in other studies. Previous reports have demonstrated SARS-CoV-2 antigens in neurospheres and brain organoids (Mesci et al., 2020; Song et al., 2020; Zhang et al., 2020) using MOIs at least 10 times higher than the MOI used in our investigation. Productive infection in neural cells, however, was only claimed at an MOI 100 times higher than the MOI used here (Zhang et al., 2020). Also, cells from lungs, intestine, heart and kidney, which have already been demonstrated to be sites of infection (Bradley et al., 2020; Mallapaty, 2020; Remmelink et al., 2020; Tabary et al., 2020), could be infected *in vitro* with MOIs ranging from 0.01 to 1 (Han et al., 2020; Lamers et al., 2020). Therefore, it seems unlikely that, in severe neuro-COVID cases such as the one described here, neural cells would be exposed to quantities equal to or more than one plaque forming virus/cell. Our observation that ChP is infected in a much greater extent than other regions of the brain, together with the lack of infectious virus particles *in vitro* with MOI < 1, argue against the clinical relevance of using high titers of SARS-CoV-2 for modeling the infection *in vitro*.

Using viral titers of MOI 0.5, it was shown that SARS-CoV-2 exclusively infects ChP cells in brain organoids, but no other cell types. Even at higher viral titers (MOI 10), infection of neurons was minor (Pellegrini et al., 2020). Our observation that SARS-CoV-2 infects the ChP without significantly spreading to other brain areas and the absence of a productive infection in human neurospheres with SARS-CoV-2 at the MOI of 0.1, corroborates these findings. Altogether, our data suggest that the human brain is likely a dead-end site for

SARS-CoV-2 replication, and that it is naturally affected by virus-triggered neuro-inflammation, justifying the neurological symptoms associated to COVID-19 (Espíndola et al., 2020; Schaller et al., 2020).

This work supports the hypothesis that the infection of ChP with SARS-CoV-2 causes impairment of the blood-CSF barrier, allowing the invasion of immune cells and the leakage of proinflammatory molecules and viral particles into the CNS. Notably, neurological symptoms are more frequent in severe patients with exacerbated inflammation, compared to mild or moderate ones, suggesting that an overall increase in the inflammatory response may set place for CNS damage (Mao et al., 2020). Low type I interferon response in infants' brains may correlate with higher susceptibility for virus entry in CNS, but also patients with previous neurological and psychiatric disorders which may have weakened immune response or enhanced inflammation should be closely monitored (Singh et al., n.d.; Mazza et al., 2020).

Acknowledgments

The authors would like to thank Claudia Figueiredo and Claudio Ferrari for helpful discussions during the elaboration of this manuscript; and Fernando Colonna Rosman and Leila Maria Cardão Chimelli for their support in the tissue's analysis. This work was supported by Conselho Nacional de Desenvolvimento Científico e Tecnológico (CNPq), Fundação de Amparo à Pesquisa do Estado do Rio de Janeiro (FAPERJ) and Coordenação de Aperfeiçoamento de Pessoal de Nível Superior (CAPES), in addition to intramural grants from the D'Or Institute for Research and Education (IDOR).

Funding was also provided by CNPq, CAPES and FAPERJ through the National Institutes of Science and Technology Program (INCT) to Carlos Morel (INCT-IDPN). Thanks are due to Oswaldo Cruz Foundation/FIOCRUZ under the auspices of Inova program (B3-Bovespa funding).

Competing interests

The authors declare no competing interests.

Materials and methods

Biological specimens

Specimens from lungs, heart and brain (frontal cortex, putamen/globus pallidus, temporal lobe, lateral ventricle, choroid plexus (ChP), cortex, midbrain, pons and medulla oblongata) from a one-year-old child deceased due to COVID-19 were obtained after a signed informed consent by the legal guardians. The study was submitted to the internal Ethics Committee approval (CAAE number: 37211220.0.0000.5249) and fully reported by Gomes and collaborators (submitted).

Total RNA isolation and virus detection in human postmortem tissues

Specimens from heart and brain (frontal cortex, LV and ChP) were sliced into thick sections, transferred to a new tube and incubated in 400 µL of lysis buffer containing 10 mM Tris-HCl pH 7.8, 1 mM EDTA, 10% SDS and 20 mg/mL Proteinase K (ThermoFisher Scientific) each. This mixture was then incubated in a water bath at 60°C for 30 minutes. Subsequently, the content was transferred to 1.5 mm TriplePure Zirconium homogenizer beads (Benchmark Scientific) and shaken vigorously using the BeadBug™ Microtube Homogenizer apparatus (D1030-E, Benchmark Scientific). The total RNA was isolated in 1 mL of TRIzol™ Reagent (ThermoFisher Scientific), according to the manufacturer's instructions. qRT–PCR was performed on each extracted sample using the 2019–nCoV CDC RUO Kit (IDT: 10006713) and 2019–nCoV CDC RUO Primers and Probes (PN: 10006713) for the detection of viral RNA (SARS-CoV-2 nucleocapsid N1 and N2 fragments) and the RNase P (RP) primer set for the detection of human RNase P RNA (Integrated DNA Technologies). For each specimen, three separated reactions were set up in a 96-well plate including N1, N2, and RP primers and probes. RT-qPCR was carried out in with a total reaction volume of 20 µL containing 15 µL of GoTaq® Probe 1-Step RT-qPCR System (Promega, A6120) comprised of the following components: 3.1 µL ultrapure water, 10 µL GoTaq® Probe qPCR Master Mix with dUTP (2X), 0.4 µL GoScriptTM RT Mix for 1-Step RT-qPCR, 1.5 µL primer/probe sets for either N1, N2, or RP (IDT) and 5 µL of extracted RNA. All reactions were carried out with appropriate negative (human specimen control – iPSC-derived astrocytes – and no template control), and positive (2019-nCoV_N Positive Control, IDT: 10006625; Hs_RPP30 Positive Control, IDT, 10006626) controls, which were incorporated into each run to ensure proper testing control. Briefly, the reactions were performed on a StepOnePlus™ Real-Time PCR System thermocycler (ThermoFisher Scientific). Thermal cycling conditions comprised a

holding stage at 45°C for 15 min, 95°C for 2 min, followed by 40 cycles of denaturation at 95°C for 15 seconds, and annealing and extension at 60°C for 1 minute.

SARS-CoV-2 propagation

SARS-CoV-2 was expanded in African green monkey kidney cells (Vero, subtype E6) from an isolate obtained from a nasopharyngeal swab from a confirmed case in Rio de Janeiro, Brazil (GenBank accession no. MT710714). Virus isolation was performed after a single passage in cell culture in a 150 cm^2 flask, previously infected with SARS-CoV-2 at MOI 0.1. Observations for cytopathic effects were performed daily and peaked 4 to 5 days after infection. All procedures related to virus culture were handled in a biosafety level 3 (BSL3) facility according to WHO guidelines. Virus stocks were kept at -80°C.

Generation of neurospheres

Human induced pluripotent stem (iPS) cells were obtained from the Coriell Institute for Medical Research repository (GM23279A) or produced in house with CytoTune™-iPS 2.0 Sendai Reprogramming Kit (A16517- Invitrogen) from skin fibroblasts (Da Silveira Paulsen et al., 2012) or urine epithelial cells (Sochacki et al., 2016). iPS cells were cultured in StemFlex media (A33494 - Thermo Fisher Scientific01) on top of Matrigel (BD Biosciences, Franklin Lakes, NJ). Neural stem cells (NSCs) were generating according to manufacturer's instructions (# MAN0008031, Life Technologies).

NSCs were cultured with neural expansion media (Advanced DMEM/F12/ Neurobasal medium 1:1, plus 1% neural induction supplement – all reagents from Thermo Fisher Scientific) on top of Geltrex LDEV-Free (Thermo Fisher Scientific, A1413302) coated plates. Upon reaching 90% of confluence, 3 x 10^6 NSCs were plated/well of 6 well-plate and cultured on an orbital shaker at 90 rpm for 7 days in standard culture conditions. The culture medium was composed of Neurobasal medium/DMEM-F12 1:1, supplemented with 1x N2 (Thermo Fisher Scientific) and 1x B27 (Thermo Fisher Scientific), and it was changed each 3-4 days (Casas et al., 2018).

Infection of neurospheres

Seven days-old neurospheres were infected with SARS-CoV-2 at MOI 0.1 (9 x 10^2 PFU per neurosphere). Following 1h incubation, the inoculum was partially replaced by fresh medium and cultured for additional 48-72h with an orbital shaking at 90 rpm in standard

conditions (5% CO_2 and 37°C). The medium was not completely replaced to avoid excessive stress to the spheres due to lack of sufficient liquid. Neurospheres exposed to uninfected Vero's culture medium were used as controls of infection (Mock). Neurospheres (≈ 50 to 200) were used per experimental group for each analysis. The assay was performed in three independent experiments, consisting of three cell lines generated from 3 independent donors.

Immunofluorescence staining

Specimens from lungs, heart and brain (frontal cortex, putamen/globus pallidus, temporal lobe, lateral ventricle, choroid plexus (ChP), cortex, midbrain, pons and medulla oblongata) were fixed in 10% neutral buffered formalin. After 48 hours, part of the samples was dehydrated in a series of increasing concentrations of ethanol, cleared in xylol and paraffin-embedded. For immunofluorescence staining, a tissue microarray (TMA) from the paraffin blocks of the above-mentioned tissues was produced by the protocol described by Pires and collaborators (Pires et al., 2006) with modifications. Some of the remaining fixed tissues were maintained in 70% ethanol before being further processed for total RNA isolation. 4 µm-sections of TMA were dewaxed with xylene and hydrated with decreasing concentrations of ethanol. Then, sections were incubated with 10 mM citrate buffer (pH 6.0) for 30 minutes for antigenic recovery, followed by incubation in permeabilization/blocking solution (0.3 % Triton X-100/ 3% bovine serum albumin, BSA, in PBS) for 2 hours. The sections were incubated in primary antibodies at 4°C overnight [anti-SARS-CoV-2 spike protein monoclonal antibody (SP) (1:500, G632604 - Genetex); anti-SARS-CoV-2 convalescent serum from a patient with COVID-19 (CS) (1:1000); and anti-double-stranded RNA (dsRNA) monoclonal antibody (J2) (1:200, MABE1134, Merck). Next, sections were incubated with the secondary antibodies: goat anti-mouse AlexaFluor 488 (1:400, A-11008 - Invitrogen) and goat anti-Human Alexa Fluor 488 (1:400; A-11013 - Invitrogen) for 1 hour. Nuclei were stained with 0.5 µg/mL 4′-6-diamino-2-phenylindole (DAPI) and the slides were mounted with Aqua-Poly/Mount (Polysciences).

For neurospheres, samples were fixed in 4% paraformaldehyde solution (Sigma-Aldrich) for 1h, followed by cryopreservation with 30% sucrose solution overnight. Then, samples were embedded in O.C.T compound (Sakura Finetek, Netherland) and frozen at -80 ˚C. The O.C.T blocks were sectioned at 20 µm slices with a Leica CM1860 cryostat. After washing with PBS, sections were incubated in permeabilization/blocking solution (0.3% Triton X-100/ 3% goat serum) for 2h. The primary antibodies were incubated overnight at 4˚C [anti-SARS-CoV-2 CS (1:1000) and anti-double-stranded RNA (dsRNA) monoclonal antibody (1:200). Then, sections were incubated with secondary antibodies (goat anti-

Human Alexa Fluor 647 and Goat anti-Mouse Alexa Fluor 488; 1:400, A21445 and A-11001 - Thermo Fisher Scientific) for 2h. Nuclei were stained with 0.5 µg/mL 40-6-diamino- 2-phenylindole (DAPI) for 10 minutes and the slides were mounted with Aqua-Poly/Mount (Polysciences).

Images of post-mortem tissues and neurospheres were acquired on a Leica TCS-SP8 confocal microscope with the 63x objective.

Plaque forming unit assay

For viral titration, monolayers of Vero E6 cells (2 x 10^4 cell/well) in 96-well plates were infected with serial dilutions of supernatants containing SARS-CoV-2 for 1 hour at 37°C. Cells were washed and 1.2% carboxymethyl cellulose (CMC)/DMEM (high glucose) semisolid medium with 2% FBS was added. At 3 days post-infection, plaque number was scored in at least 3 replicates per dilution by independent readers. The reader was blind with respect to the source of the supernatant.

Molecular detection of virus RNA

The total RNA from neurosphere's supernatant was extracted using QIAamp Viral RNA (Qiagen), according to manufacturer's instructions. Quantitative RT-PCR was performed using QuantiTect Probe RT-PCR Kit (Quiagen®) in an ABI PRISM 7500 Sequence Detection System (Applied Biosystems). Amplifications were carried out in 25 µL reaction mixtures containing 2X reaction mix buffer, 50 µM of each primer, 10 µM of probe, and 5 µL of RNA template. Primers, probes, and cycling conditions recommended by the Centers for Disease Control and Prevention (CDC) protocol were used to detect the SARS-CoV-2 (https://www.fda.gov). The standard curve method was employed for virus quantification. For reference to the cell amounts used, the housekeeping gene RNAse P was amplified. The Ct values for this target were compared to those obtained to different cell amounts, 10^7 to 10^2, for calibration.

Western blot analysis

After 2 days post-infection (d.p.i), 100 µL of sample buffer without bromophenol blue (62.5 mM Tris-HCl, pH 6.8, containing 10% glycerol, 2% SDS and 5% 2-mercaptoethanol) was added to the neurospheres and, then, frozen at -80°C. Next, samples were gently digested with a disposable pestle (BAF 199230001- Sigma, Bel-Art) and cell extracts were

boiled at 95°C for 10 min and centrifuged at 4°C 16000 g for 15 min to remove insoluble material. Protein content was estimated using the Bio-Rad Protein Assay (#5000006, Biorad). After addition of bromophenol blue (0.02%), extract samples (40 µg/lane for neurospheres and 15 µg/lane for Vero cells) were separated by electrophoresis on a 10% SDS polyacrylamide gel and transferred to polyvinylidene difluoride (PVDF) membranes. Western blotting was performed with minor modifications from the originally described (Towbin et al., 1989). Membranes were blocked in 5% non-fat milk in Tris-Buffered Saline with 0.1% Tween-20 (TBS-T) for 1 hour at room temperature. Membranes were then incubated overnight at 4°C, in the presence of anti-SARS-CoV-2 CS (1:5,000), anti SARS-CoV-2 SP (1:2,000, #GTX632604 - GeneTex) and anti-actin (1:2000, MAB1501, Millipore) diluted in TBS-T with 5% non-fat milk. Then, membranes were incubated with peroxidase-conjugated antibodies: goat anti-Human IgG, HRP (1:4,000, 62-8420 - Invitrogen) and goat anti-Mouse IgG (H+L), HRP-conjugate (1:10,000, G21040 -Molecular Probes). The signals were developed using ECL Prime Western Blotting System (#GERPN2232, Sigma) for five minutes and chemiluminescence was detected with an Odyssey-FC System® (Imaging System - LI-COR Biosciences). For this purpose, membranes were incubated for three cycles of 10 minutes in stripping buffer (pH 2.2, 200 mM glycine, SDS 0,1% and 1% Tween-20), the buffer was discarded, the membranes were washed for 5 minutes with PBS (three times) and 5 minutes with 0.1% TBS-T (three times). Next, the membranes were blocked again and processed for immunolabeling as described above.

Total RNA isolation from human cells and cDNA synthesis

Neurospheres grown for 7 days in agitation in 6-well plates, were collected, pelleted and frozen immediately at -80°C until further processing. Total RNA isolation was performed using ReliaPrep™ RNA Tissue Miniprep System (Promega Corporation) according to manufacturer's instructions. For cardiomyocytes, total RNA was isolated using TRIzol™ reagent, according to manufacturer's recommendations (Thermo Fisher Scientific). Subsequently, RNA concentration and quality were quantified on a NanoDrop™ 2000c Spectrophotometer (Thermo Fisher Scientific) and integrity and purity were evaluated by 1.8% agarose gel electrophoresis using a photodocumentation device equipped with a UV lamp (L-PIX, Loccus Biotecnologia). After isolation, total RNA was digested with DNase I, Amplification Grade, following the manufacturer's instructions (Invitrogen, Thermo Fisher Scientific). From DNAse-treated samples, 2 µg of RNA were reverse transcribed using M-MLV for complementary DNA generation (cDNA) (Thermo Fisher Scientific).

Gene expression analysis by real time qRT-PCR

Quantitative RT-PCR reactions were conducted in three replicates with a final reaction volume of 10 µL in MicroAmp Fast Optical 96 Well Reaction Plates (Thermo Fisher Scientific) containing 1X GoTaq qPCR Master Mix (Promega Corporation), 300 nM CXR Reference Dye, a final concentration of 200 nM of each SYBR green designed primers [Angiotensin I Converting Enzyme 2 (ACE2; forward: 5'-CGAAGCCGAAGACCTGTTCTA-3'; reverse: 5'-GGGCAAGTGTGGACTGTTCC-3') ThermoFisher Scientific] and 10 ng of cDNA per reaction. Appropriate controls (no reverse transcriptase and template-negative controls) were incorporated into each run. Briefly, the reactions were performed on a StepOnePlus™ Real-Time PCR System thermocycler (Applied Biosystems). Thermal cycling program comprised hold stage at 95°C for 3 min, followed by 40 cycling stages at 95°C for 15 sec, 57°C for 15 sec, 72°C for 15 sec and melt curve stage 95 °C, 15 sec; 60 °C, 1 min; 95 °C, 15 sec. The relative expression of the genes of interest was normalized by human reference genes: Glyceraldehyde-3-phosphate Dehydrogenase (GAPDH; forward: 5'-GCCCTCAACGACCACTTTG-3'; reverse: 5'-CCACCACCCTGTTGCTGTAG-3') and Hypoxanthine Phosphoribosyltransferase 1 (HPRT-1; forward 5'-CGTCGTGATTAGTGATGATGAACC-3'; reverse: 5'-AGAGGGCTACAATGTGATGGC-3'). qPCR data analysis was performed with the N_0 method implemented in LinRegPCR v. 2020.0, which considers qPCR mean efficiencies estimated by the window-of-linearity method (Ramakers et al., 2003; Ruijter et al., 2009). Summarily, N_0 values were calculated in LinRegPCR using default parameters. Then, arithmetic mean of N_0 values from gene of interest (GOI) were normalized by taking its ratio to the N_0 geometric mean of the reference genes (REF) *GAPDH and HRRT-1* (N_{0GOI}/N_{0REF}).

References

Annweiler C, Cao Z, Wu Y, Faucon E, Mouhat S, Kovacic H, Sabatier J-M (2020) Counter-regulatory “Renin-Angiotensin” System-based Candidate Drugs to Treat COVID-19 Diseases in SARS-CoV-2-infected patients. Infect Disord Drug Targets.

Bradley BT, Maioli H, Johnston R, Chaudhry I, Fink SL, Xu H, Najafian B, Deutsch G, Lacy JM, Williams T, Yarid N, Marshall DA (2020) Histopathology and ultrastructural findings of fatal COVID-19 infections in Washington State: a case series. Lancet 396:320–332.

Brann DH et al. (2020) Non-neuronal expression of SARS-CoV-2 entry genes in the olfactory system suggests mechanisms underlying COVID-19-associated anosmia. Science Advances 6:eabc5801.

Bryche B, Albin AS, Murri S, Lacôte S, Pulido C, Gouilh MA, Lesellier S, Servat A, Wasniewski M, Picard-Meyer E, Monchatre-Leroy E, Volmer R, Rampin O, Goffic RL, Marianneau P, Meunier N (2020) Massive transient damage of the olfactory epithelium associated with infection of sustentacular cells by SARS-CoV-2 in golden Syrian hamsters. bioRxiv:2020.06.16.151704.

Casas BS, Vitória G, do Costa MN, Madeiro da Costa R, Trindade P, Maciel R, Navarrete N, Rehen SK, Palma V (2018) hiPSC-derived neural stem cells from patients with schizophrenia induce an impaired angiogenesis. Translational Psychiatry 8:1–15.

Da Silveira Paulsen B, De Moraes Maciel R, Galina A, Da Silveira MS, Souza CDS, Drummond H, Pozzatto EN, Junior HS, Chicaybam L, Massuda R, Setti-Perdigão P, Bonamino M, Belmonte-De-Abreu PS, Castro NG, Brentani H, Rehen SK (2012) Altered Oxygen Metabolism Associated to Neurogenesis of Induced Pluripotent Stem Cells Derived from a Schizophrenic Patient. Cell Transplant 21:1547–1559.

De Felice FG, Tovar-Moll F, Moll J, Munoz DP, Ferreira ST (2020) Severe Acute Respiratory Syndrome Coronavirus 2 (SARS-CoV-2) and the Central Nervous System. Trends Neurosci 43:355–357.

Ellul MA, Benjamin L, Singh B, Lant S, Michael BD, Easton A, Kneen R, Defres S, Sejvar J, Solomon T (2020) Neurological associations of COVID-19. The Lancet Neurology 19:767–783.

Espíndola O de M, Siqueira M, Soares CN, Lima MASD de, Leite ACCB, Araujo AQC, Brandão CO, Silva MTT (2020) Patients with COVID-19 and neurological manifestations show undetectable SARS-CoV-2 RNA levels in the cerebrospinal fluid. International Journal of Infectious Diseases 96:567–569.

Fifi JT, Mocco J (2020) COVID-19 related stroke in young individuals. The Lancet Neurology 19:713–715.

Garcez PP, Loiola EC, Costa RM da, Higa LM, Trindade P, Delvecchio R, Nascimento JM, Brindeiro R, Tanuri A, Rehen SK (2016) Zika virus impairs growth in human neurospheres and brain organoids. Science 352:816–818.

Garcez PP, Nascimento JM, de Vasconcelos JM, Madeiro da Costa R, Delvecchio R, Trindade P, Loiola EC, Higa LM, Cassoli JS, Vitória G, Sequeira PC, Sochacki J, Aguiar RS, Fuzii HT, de Filippis AMB, da Silva Gonçalves Vianez Júnior JL, Tanuri A, Martins-de-Souza D, Rehen SK (2017) Zika virus disrupts molecular fingerprinting of human neurospheres. Sci Rep 7:40780.

Glass WG, Subbarao K, Murphy B, Murphy PM (2004) Mechanisms of host defense following severe acute respiratory syndrome-coronavirus (SARS-CoV) pulmonary infection of mice. J Immunol 173:4030–4039.

Hamming I, Timens W, Bulthuis M, Lely A, Navis G, van Goor H (2004) Tissue distribution of ACE2 protein, the functional receptor for SARS coronavirus. A first step in understanding SARS pathogenesis. J Pathol 203:631–637.

Han Y et al. (2020) Identification of Candidate COVID-19 Therapeutics using hPSC-derived Lung Organoids. bioRxiv:2020.05.05.079095.

Jacob F, Pather SR, Huang W-K, Wong SZH, Zhou H, Zhang F, Cubitt B, Chen CZ, Xu M, Pradhan M, Zhang DY, Zheng W, Bang AG, Song H, Torre JC de a, Ming G (2020) Human Pluripotent Stem Cell-Derived Neural Cells and Brain Organoids Reveal SARS-CoV-2 Neurotropism. bioRxiv:2020.07.28.225151.

Javed K, Reddy V, Lui F (2020) Neuroanatomy, Choroid Plexus. In: StatPearls. Treasure Island (FL): StatPearls Publishing. Available at: http://www.ncbi.nlm.nih.gov/books/NBK538156/ [Accessed September 3, 2020].

Kim J, Alejandro B, Hetman M, Hattab EM, Joiner J, Schroten H, Ishikawa H, Chung D-H (2020) Zika virus infects pericytes in the choroid plexus and enters the central nervous system through the blood-cerebrospinal fluid barrier. PLOS Pathogens 16:e1008204.

Lamers MM et al. (2020) SARS-CoV-2 productively infects human gut enterocytes. Science 369:50–54.

Li K, Wohlford-Lenane C, Perlman S, Zhao J, Jewell AK, Reznikov LR, Gibson-Corley KN, Meyerholz DK, McCray PB (2016) Middle East Respiratory Syndrome Coronavirus Causes Multiple Organ Damage and Lethal Disease in Mice Transgenic for Human Dipeptidyl Peptidase 4. J Infect Dis 213:712–722.

Liu M, Wang T, Zhou Y, Zhao Y, Zhang Y, Li J (2020) Potential Role of ACE2 in Coronavirus Disease 2019 (COVID-19) Prevention and Management. J Transl Int Med 8:9–19.

Lun MP, Monuki ES, Lehtinen MK (2015) Development and functions of the choroid plexus–cerebrospinal fluid system. Nature Reviews Neuroscience 16:445–457.

Mallapaty S (2020) Mini organs reveal how the coronavirus ravages the body. Nature 583:15–16.

Mao L, Wang M, Chen S, He Q, Chang J, Hong C, Zhou Y, Wang D, Li Y, Jin H, Hu B (2020) Neurological Manifestations of Hospitalized Patients with COVID-19 in Wuhan, China: a retrospective case series study. medRxiv:2020.02.22.20026500.

Marchiano S, Hsiang T-Y, Higashi T, Khanna A, Reinecke H, Yang X, Pabon L, Sniadecki NJ, Bertero A, Gale M, Murry CE (2020) SARS-CoV-2 infects human pluripotent stem cell-derived cardiomyocytes, impairing electrical and mechanical function. bioRxiv:2020.08.30.274464.

Mazza MG, De Lorenzo R, Conte C, Poletti S, Vai B, Bollettini I, Melloni EMT, Furlan R, Ciceri F, Rovere-Querini P, Benedetti F (2020) Anxiety and depression in COVID-19 survivors: Role of inflammatory and clinical predictors. Brain, Behavior, and Immunity Available at: http://www.sciencedirect.com/science/article/pii/S0889159120316068 [Accessed August 26, 2020].

Meng H, Xiong R, He R, Lin W, Hao B, Zhang L, Lu Z, Shen X, Fan T, Jiang W, Yang W, Li T, Chen J, Geng Q (2020) CT imaging and clinical course of asymptomatic cases with COVID-19 pneumonia at admission in Wuhan, China. J Infect 81:e33–e39.

Mesci P, Macia A, Saleh A, Martin-Sancho L, Yin X, Snethlage C, Avansini S, Chanda SK, Muotri A (2020) Sofosbuvir protects human brain organoids against SARS-CoV-2. bioRxiv:2020.05.30.125856.

O'Hara BA, Morris-Love J, Gee GV, Haley SA, Atwood WJ (2020) JC Virus infected choroid plexus epithelial cells produce extracellular vesicles that infect glial cells independently of the virus attachment receptor. PLOS Pathogens 16:e1008371.

Pellegrini L, Albecka A, Mallery DL, Kellner MJ, Paul D, Carter AP, James LC, Lancaster MA (2020) SARS-CoV-2 infects brain choroid plexus and disrupts the blood-CSF-barrier. bioRxiv:2020.08.20.259937.

Pérez-Bermejo JA, Kang S, Rockwood SJ, Simoneau CR, Joy DA, Ramadoss GN, Silva AC, Flanigan WR, Li H, Nakamura K, Whitman JD, Ott M, Conklin BR, McDevitt TC (2020) SARS-CoV-2 infection of human iPSC-derived cardiac cells predicts novel cytopathic features in hearts of COVID-19 patients. bioRxiv:2020.08.25.265561.

Pinto BGG, Oliveira AER, Singh Y, Jimenez L, Gonçalves ANA, Ogava RLT, Creighton R, Schatzmann Peron JP, Nakaya HI (2020) ACE2 Expression Is Increased in the Lungs of Patients With Comorbidities Associated With Severe COVID-19. J Infect Dis 222:556–563.

Pires ARC, Andreiuolo F da M, de Souza SR (2006) TMA for all: a new method for the construction of tissue microarrays without recipient paraffin block using custom-built needles. Diagnostic Pathology 1:14.

Qian X et al. (2016) Brain-Region-Specific Organoids Using Mini-bioreactors for Modeling ZIKV Exposure. Cell 165:1238–1254.

Ramakers C, Ruijter JM, Deprez RHL, Moorman AFM (2003) Assumption-free analysis of quantitative real-time polymerase chain reaction (PCR) data. Neurosci Lett 339:62–66.

Remmelink M, De Mendonça R, D'Haene N, De Clercq S, Verocq C, Lebrun L, Lavis P, Racu M-L, Trépant A-L, Maris C, Rorive S, Goffard J-C, De Witte O, Peluso L, Vincent J-L, Decaestecker C, Taccone FS, Salmon I (2020) Unspecific post-mortem findings despite multiorgan viral spread in COVID-19 patients. Crit Care

24 Available at: https://www.ncbi.nlm.nih.gov/pmc/articles/PMC7422463/ [Accessed August 26, 2020].

Rocha NP, Simoes E Silva AC, Prestes TRR, Feracin V, Machado CA, Ferreira RN, Teixeira AL, de Miranda AS (2018) RAS in the Central Nervous System: Potential Role in Neuropsychiatric Disorders. Curr Med Chem 25:3333–3352.

Ruijter JM, Ramakers C, Hoogaars WMH, Karlen Y, Bakker O, van den Hoff MJB, Moorman AFM (2009) Amplification efficiency: linking baseline and bias in the analysis of quantitative PCR data. Nucleic Acids Res 37:e45.

Schaller T, Hirschbühl K, Burkhardt K, Braun G, Trepel M, Märkl B, Claus R (2020) Postmortem Examination of Patients With COVID-19. JAMA 323:2518–2520.

Schwerk C, Tenenbaum T, Kim KS, Schroten H (2015) The choroid plexus—a multi-role player during infectious diseases of the CNS. Front Cell Neurosci 9 Available at: https://www.frontiersin.org/articles/10.3389/fncel.2015.00080/full [Accessed August 26, 2020].

Singh AK, Bhushan B, Maurya A, Mishra G, Singh SK, Awasthi R (n.d.) Novel coronavirus disease 2019 (COVID-19) and neurodegenerative disorders. Dermatologic Therapy n/a:e13591.

Sochacki J, Devalle S, Reis M, Mattos P, Rehen S (2016) Generation of urine iPS cell lines from patients with Attention Deficit Hyperactivity Disorder (ADHD) using a non-integrative method. Stem Cell Res 17:102–106.

Song E et al. (2020) Neuroinvasive potential of SARS-CoV-2 revealed in a human brain organoid model. bioRxiv:2020.06.25.169946.

Sungnak W, Huang N, Bécavin C, Berg M, Queen R, Litvinukova M, Talavera-López C, Maatz H, Reichart D, Sampaziotis F, Worlock KB, Yoshida M, Barnes JL (2020) SARS-CoV-2 entry factors are highly expressed in nasal epithelial cells together with innate immune genes. Nature Medicine 26:681–687.

Tabary M, Khanmohammadi S, Araghi F, Dadkhahfar S, Tavangar SM (2020) Pathologic features of COVID-19: A concise review. Pathol Res Pract 216:153097.

Wang L, Shen Y, Li M, Chuang H, Ye Y, Zhao H, Wang H (2020) Clinical manifestations and evidence of neurological involvement in 2019 novel coronavirus SARS-CoV-2: a systematic review and meta-analysis. J Neurol:1–13.

Wilcox DR, Folmsbee SS, Muller WJ, Longnecker R (2016) The Type I Interferon Response Determines Differences in Choroid Plexus Susceptibility between Newborns and Adults in Herpes Simplex Virus Encephalitis. mBio 7 Available at: https://www.ncbi.nlm.nih.gov/pmc/articles/PMC4959527/ [Accessed September 2, 2020].

Xu J, Zhong S, Liu J, Li L, Li Y, Wu X, Li Z, Deng P, Zhang J, Zhong N, Ding Y, Jiang Y (2005) Detection of Severe Acute Respiratory Syndrome Coronavirus in the Brain: Potential Role of the Chemokine Mig in Pathogenesis. Clin Infect Dis 41:1089–1096.

Yan R, Zhang Y, Li Y, Xia L, Guo Y, Zhou Q (2020) Structural basis for the recognition of SARS-CoV-2 by full-length human ACE2. Science 367:1444–1448.

Zhang B-Z, Chu H, Han S, Shuai H, Deng J, Hu Y, Gong H, Lee AC-Y, Zou Z, Yau T, Wu W, Hung IF-N, Chan JF-W, Yuen K-Y, Huang J-D (2020) SARS-CoV-2 infects human neural progenitor cells and brain organoids. Cell Research:1–4.